Original Article

A novel prediction tool based on shear wave elastography, gallbladder ultrasound, and serum biomarkers for the early diagnosis of biliary atresia in infants younger than 60 days old

Hualin Yan[1]^, Juxian Liu[1]^, Shuguang Jin[2], Lanxin Du[3], Qi Wang[2], Yan Luo[1]

[1]Department of Medical Ultrasound, West China Hospital, Sichuan University, Chengdu, China; [2]Department of Pediatric Surgery, West China Hospital, Sichuan University, Chengdu, China; [3]Department of Ultrasound, West China Second University Hospital, Sichuan University, Chengdu, China

Contributions: (I) Conception and design: H Yan, J Liu, S Jin; (II) Administrative support: J Liu, S Jin; (III) Provision of study materials or patients: L Du, Q Wang; (IV) Collection and assembly of data: Y Luo, L Du; (V) Data analysis and interpretation: L Du, Q Wang, Y Luo; (VI) Manuscript writing: All authors; (VII) Final approval of manuscript: All authors.

Correspondence to: Juxian Liu. Department of Medical Ultrasound, West China Hospital, Sichuan University, Chengdu 610041, China; Email: liujuxian@wchscu.cn; Shuguang Jin. Department of Pediatric Surgery, West China Hospital, Sichuan University, Chengdu 610041, China. Email: shgjin2003@aliyun.com.

Background: Early Kasai surgery before 60 days of life results in better clinical outcomes in patients with biliary atresia (BA). We aimed to develop and validate a prediction tool for the early diagnosis of BA in infants younger than 60 days old.

Methods: This prospective study recruited consecutive infants younger than 60 days old with conjugated hyperbilirubinemia who were evaluated with an ultrasound (US) scan, including B-mode US with color Doppler flow imaging (CDFI) features and liver two-dimensional shear wave elastography (2D SWE), from March 2017 to July 2021. The reference standard for diagnosis was intraoperative cholangiography, liver biopsy, or the resolution of jaundice. Area under the receiver operating characteristic curve (AUC) analysis, logistic regression analysis, and establishment of a nomogram were performed.

Results: A total of 174 patients (mean age, 46 days), including 87 infants with BA and 87 non-BA cholestatic infants, were included in the study. The established nomogram based on gallbladder (GB) abnormality, liver 2D SWE, and serum γ-glutamyl transferase (GGT) and alanine aminotransferase (ALT) had an AUC of 0.99 [95% confidence interval (CI): 0.94–1.00], a sensitivity of 92%, and a specificity of 100%. The nomogram in the validation cohort also had good diagnostic performance in the diagnosis of BA, with an AUC of 0.98 (95% CI: 0.95–1.00).

Conclusions: The new prediction tool had a good diagnostic performance in the early prediction of BA in infants younger than 60 days old and will facilitate timely Kasai surgery.

Keywords: Biliary atresia (BA); nomogram; diagnosis; ultrasound (US); shear wave elastography (SWE)

Submitted Apr 05, 2022. Accepted for publication Sep 20, 2022. Published online Oct 13, 2022.
doi: 10.21037/qims-22-324
View this article at: https://dx.doi.org/10.21037/qims-22-324

^ ORCID: Hualin Yan, 0000-0003-1338-1124; Juxian Liu, 0000-0002-5315-5482.

Introduction

Biliary atresia (BA) is a rare disease involving the intrahepatic and extrahepatic bile ducts that presents as persistent neonatal cholestasis and progressive liver fibrosis and cirrhosis. The incidence of BA is 0.73–1.51 per 10,000 live births (1,2). Currently, BA remains the most common indication for pediatric liver transplantation (3). Without surgical treatment, patients with BA die in the first 2 years of life (4). Kasai hepatic portoenterostomy is the standard treatment for BA, and early Kasai surgery before 60 days of life results in a higher survival rate with native liver and better long-term clinical outcomes (5,6). Intraoperative cholangiography is the reference standard for BA diagnosis but is an invasive procedure (7). Timely noninvasive diagnosis of BA, especially at less than 60 days of age, remains challenging in infants with cholestasis caused by various other diseases, such as idiopathic neonatal hepatitis.

Ultrasound (US) is recommended for BA diagnosis by the North American Society for Pediatric Gastroenterology, Hepatology, and Nutrition guidelines (7). The triangular cord (TC) sign and abnormal gallbladder (GB) morphology are the most frequently reported US features in identifying BA (8-11). However, it is challenging to diagnose BA in infants younger than 60 days old because the TC sign is less common and while abnormalities are more difficult to detect in young patients with BA (12).

Two-dimensional shear wave elastography (2D SWE) is a new imaging modality in the noninvasive assessment of liver fibrosis (13). As there is progressive liver fibrosis and cirrhosis in BA, 2D SWE has been proposed for the diagnosis of BA. Compared with the METAVIR liver fibrosis score, liver SWE values significantly correlate with the stage of liver fibrosis and can assess the liver fibrosis not only in patients with BA but also in those without BA who have chronic liver diseases (14,15). However, 2 recent studies showed that the diagnostic performance of 2D SWE in predicting BA had an area under the receiver operating characteristic curve (AUC) of 0.74 to 0.79 (16,17), which was inferior to the that of B-mode US-derived features. The AUC of liver SWE in identifying BA has been reported as even lower in young infants with BA (17). Sandberg *et al.* (17) suggested that SWE is useful in the setting of equivocal B-mode US findings, and they proposed a flowchart to predict BA. Chen *et al.* (18) also combined the TC sign, GB abnormalities, serum γ-glutamyl transferase (GGT), and elastography to generate a 3-color risk stratification tool for BA diagnosis. The combination of B-mode US, liver SWE, and laboratory findings has improved the performance of BA diagnosis. However, the current combined tools are complex and difficult to implement in clinical practice. Improvement of the diagnostic accuracy for young patients in BA will facilitate timely Kasai surgery.

Here, we conducted a prospective diagnostic study to develop and validate a novel prediction tool for distinguishing BA from other causes of neonatal cholestasis in patients younger than 60 days old. In this study, we investigated different clinical and US parameters, such as age, sex, serum GGT and alanine aminotransferase (ALT), B-mode US with color Doppler flow imaging (CDFI), pulse wave (PW) Doppler US features, and liver 2D SWE, to generate an optimized nomogram for the early diagnosis of BA in infants younger than 60 days old. We present the following article in accordance with the STARD reporting checklist (available at https://qims.amegroups.com/article/view/10.21037/qims-22-324/rc).

Methods

Ethical approval

This single-center, prospective study was approved by the institutional review board of West China Hospital, Sichuan University, and written informed parental or guardians' consent was provided by all included participants. The study was conducted in accordance with the Declaration of Helsinki (as revised in 2013).

Patients and study design

For the training cohort, from March 2017 to July 2021, a total of 236 consecutive infants aged less than 60 days with conjugated hyperbilirubinemia [serum direct bilirubin >17 μmol/L and a direct to total bilirubin ratio >20% (19)] were evaluated with a US scan. Serum liver function tests, including GGT, ALT, aspartate aminotransferase (AST), alkaline phosphatase (ALP), and albumin, were collected within 1 week before US examination. The reference standard diagnosis was intraoperative cholangiography, liver biopsy, or the resolution of jaundice. A total of 62 patients were excluded for the following reasons: loss to follow-up (n=20) or with an unclear final diagnosis (n=42, including 16 patients who died during follow-up, 10 patients with abandoned treatment, and 16 patients who did not recover after nonoperative treatment). Finally, 174 infants were included in the study (*Figure 1*). Among them, 104 infants were in the training cohort, and 70 infants were in the validation cohort.

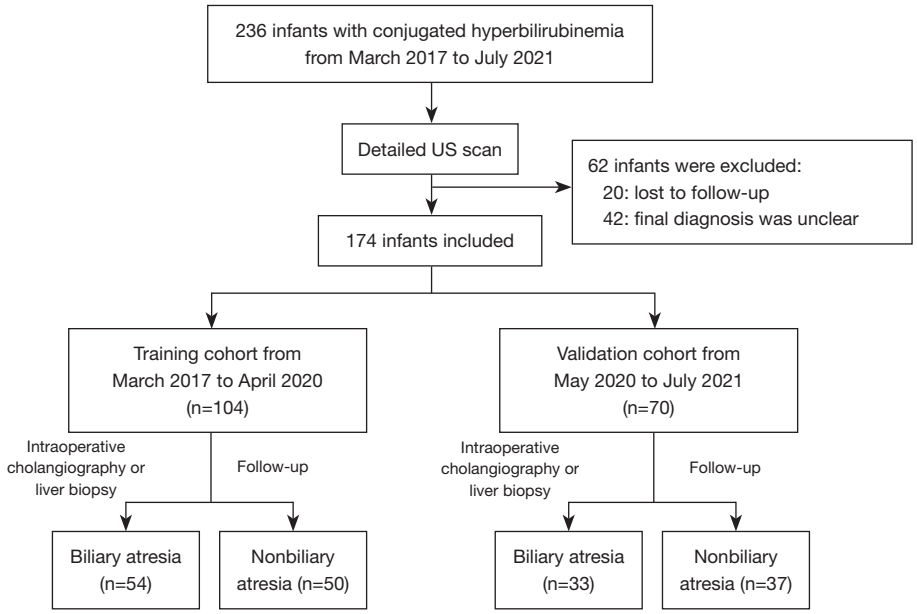

Figure 1 Flow diagram of the study design. US, ultrasound.

US examination

All included patients underwent a US examination performed by J.L or H.Y., each with more than 5 years of experience in pediatric US. An AixPlorer scanner (Supersonic Imagine, Aix-en-Province, France) incorporating a 4- to 15-MHz linear transducer and a 1- to 6-MHz curved transducer was used. The US examination protocol was as follows:

(I) Determination of GB abnormality (*Figure 2*). Infants fasted for at least 4 hours. An abnormal GB was defined by one of the following US findings: absence of GB, GB with a filled lumen and a length up to 1.5 cm (*Figure 2A*), GB with a filled lumen and a length over 1.5 cm but a length to width ratio over 5.2, or GB with an incompletely filled lumen and stiff and coarse inner wall (*Figure 2A*,*2B*) (9,11,20). A GB found to have an incompletely filled lumen but with a smooth and completely hyperechogenic mucosal lining was considered normal (*Figure 2C*) (9).

(II) The TC thickness measurement. TC thickness was defined as the thickness of the echogenic anterior wall of the anterior branch of the right portal vein (PV) just distal to the right PV in a transverse oblique plane (8,9).

(III) PV, hepatic artery (HA), and splenic vein (SV) diameter measurements. PV and HA diameters were measured at the oblique plane of the main PV or main HA from the inner wall to the inner wall and perpendicular to the wall. The SV diameter was measured at the longitudinal coronal plane of the spleen.

(IV) Right liver lobe size measurement. The maximum oblique diameter of the right lobe of the liver was measured at the plane of the right hepatic vein with a curvilinear transducer.

The CDFI and PW Doppler examination protocols were as follows:

(I) HA resistive index (HARI) measurement. Pulsed HA was first found at the oblique plane of the right liver lobe. The following formula was used to calculate HARI: HARI = (peak systolic velocity – end-diastolic velocity)/peak systolic velocity.

(II) Hepatic subcapsular flow. Vascular structures continuing to the liver capsular surface on CDFI was considered to indicate the presence of hepatic subcapsular flow (21).

Liver 2D SWE examination

A linear array AixPlorer scanner (Supersonic Imagine) was used. Segments V or VI were selected for measurement. Liver 2D SWE was performed by J.L or H.Y., each

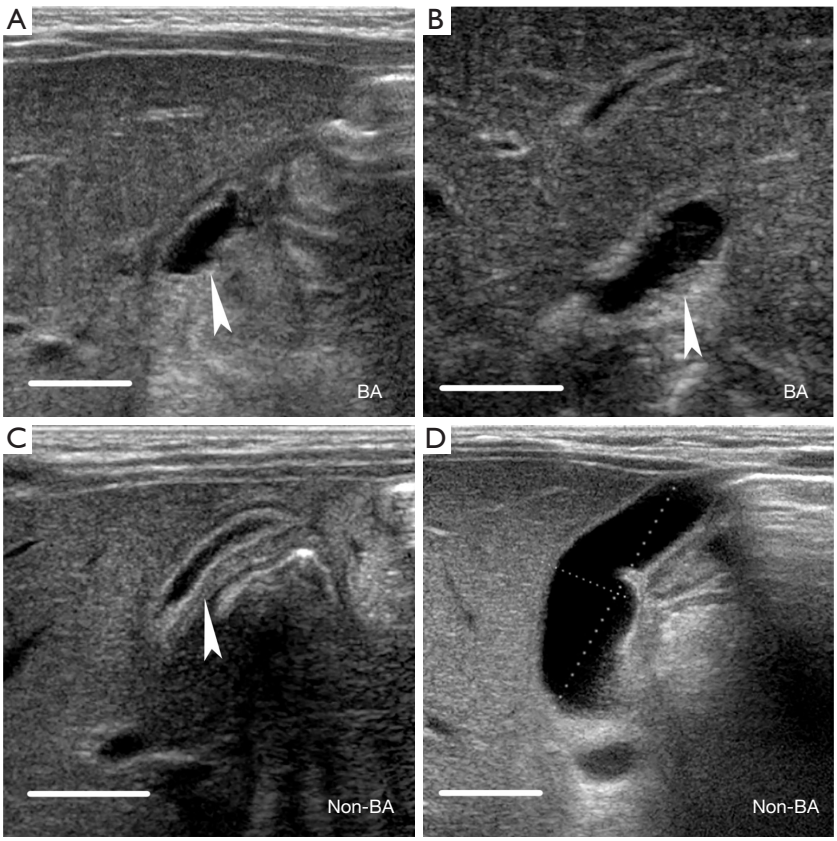

Figure 2 Longitudinal B-mode US images of gallbladder. (A) A 56-day-old girl with BA. US shows an abnormal gallbladder (arrowhead) 1.1 cm in length and a stiff and coarse inner wall. (B) A 55-day-old girl with BA. US shows an abnormal gallbladder (arrowhead) with a stiff and coarse inner wall. (C) A 23-day-old boy without BA. US shows a normal gallbladder (arrowhead) with an incompletely filled lumen but with a smooth and completely hyperechogenic mucosal lining. (D) A 55-day-old boy without BA. US shows a normal gallbladder 3.9 cm in length and 1.1 cm in width (calipers). Scale bar =1 cm. US, ultrasound; BA, biliary atresia.

with more than 3 years of experience in elastography. A rectangular region of interest (ROI) was placed over an isoechoic area of liver parenchyma, with vessels, nodules, or other structures being avoided. The analysis box was set to hepatic subcapsular 5–10 mm. A successful measurement was defined as when most of the ROI box was filled with homogeneous color and maintained for at least 1 respiratory cycle. The mean value of the ROI was recorded (*Figure 3*). The measurement was repeated at least 3 times, and an interquartile range ≤30% of the median was required to ensure reliability (16,22).

Tests of intraobserver and interobserver reliability

A total of 30 patients were randomly selected to test the intraobserver and interobserver reliability of the measurement of GB abnormality, TC thickness, and liver 2D SWE. Both operators were blinded to the liver biopsy results and the final diagnosis of the patients.

Follow-up and histology

For all the included inpatients, basic characteristics such as age, sex, and the results of serum liver function tests were recorded. The intraoperative cholangiography results, Kasai surgery details, and liver biopsy results were also collected. For outpatients, the serum markers at follow-up were recorded. When the level of serum bilirubin decreased to a normal level during follow-up or the patient was diagnosed by a pediatrician with other diseases, such as Alagille syndrome, the patients were included in the non-BA group (*Figure 1*).

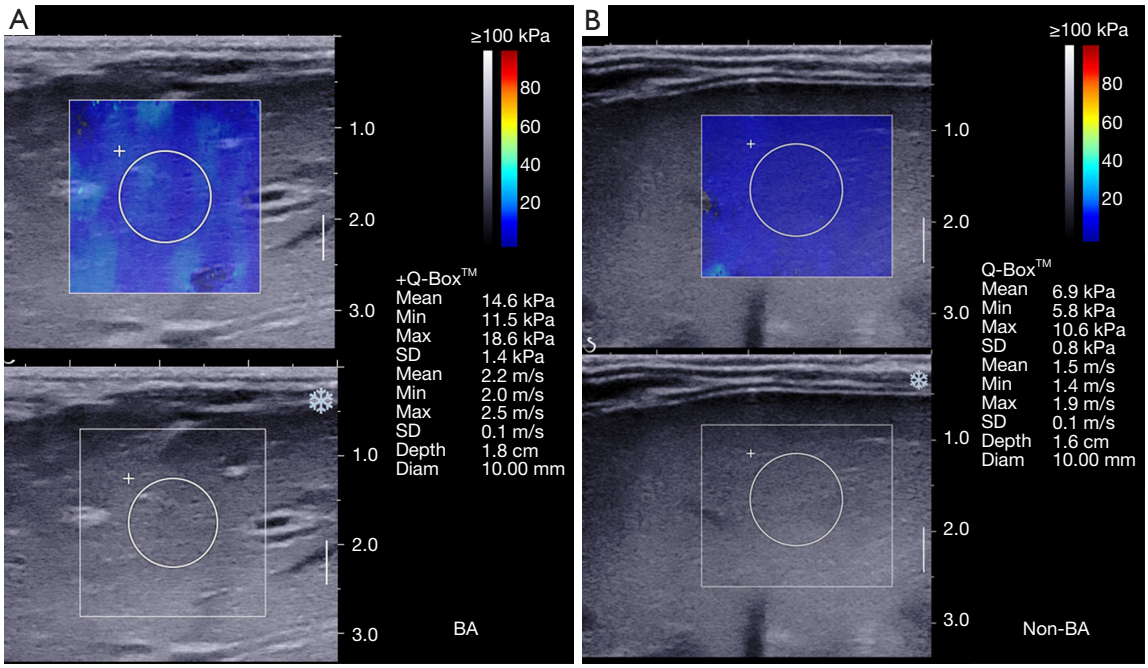

Figure 3 Shear wave elastography measurement: (A) A 37-day-old girl with biliary atresia: the measurement in the regions of interest is 14.6 kPa. (B) A 30-day-old boy without biliary atresia: the measurement in the regions of interest is 6.9 kPa. SD, standard deviation; Diam, diameter; BA, biliary atresia.

Statistical analysis

SPSS 25.0 (IBM Corp., Armonk, NY, USA) and R 4.0.5. (R Foundation for Statistical Computing, Vienna, Austria) software were used for statistical analysis. Continuous variables were compared using Student's *t*-test or the Mann-Whitney test, and categorical variables were compared using the χ^2 test. For the intraobserver and interobserver variability tests, the intraclass correlation coefficient (ICC), kappa statistic and Bland-Altman plots were used. Receiver operating characteristic (ROC) curves were constructed to compare the diagnostic performance of different US parameters in distinguishing BA from non-BA. The cutoff value of each parameter in the AUC was determined by the largest Youden index. The comparison of different AUCs was performed using DeLong's test. The corresponding sensitivity, specificity, positive predictive value (PPV), negative predictive value (NPV), and accuracy of each US parameter were calculated. Multivariable logistic regression analyses were performed to incorporate all the significant parameters and establish the prediction model using backward step-down selection. A nomogram of the training cohort was established. The AUCs were used to compare the performance of the nomogram to that of other single parameters. A calibration curve was generated to explore the performance characteristics of the nomogram. Decision curve analysis (DCA) was conducted to assess the clinical utility of the nomogram at different predicted probabilities. An external validation of the nomogram performance was carried out on the validation cohort. A P value <0.05 was considered statistically significant.

Results

Patient characteristics

After the final diagnosis was confirmed by intraoperative cholangiography or follow-up, we included 104 infants (54 BA and 50 non-BA) in the training cohort and 70 infants (33 BA and 37 non-BA) in the validation cohort. The mean age was 46 days, and 84 (48%) male infants were included. No significant difference in age or sex ratio was found between the BA and non-BA groups. According to the cholangiography results, patients with BA were classified into 3 Kasai types: type I, atresia of the common bile duct; type II, atresia of the hepatic duct; and type III, atresia of the bile duct at the porta hepatis. Most patients with BA were Kasai type III, with 48 in the training cohort and 29 in

Table 1 Patient characteristics at the time of US examination

Characteristic	Training cohort			Validation cohort		
	BA group (n=54)	Non-BA group (n=50)	P value	BA group (n=33)	Non-BA group (n=37)	P value
Age (d)†	47±10 [18–60]	43±15 [2–60]	0.060	49±9 [18–60]	47±13 [7–60]	0.496
Sex [%]‡			0.433			0.641
Male	24 [44]	27 [54]		15 [45]	18 [49]	
Female	30 [56]	23 [46]		18 [55]	19 [51]	
Kasai type [%]‡						0.951§
Type I	2 [4]	N/A		1 [3]	N/A	
Type II	4 [7]	N/A		3 [10]	N/A	
Type III	48 [89]	N/A		29 [87]	N/A	
Total bilirubin level (μmol/L)†	180.4±50.5	145.7±82.5	0.016	190.4±71.7	162.8±91.7	0.189
Direct bilirubin level (μmol/L)†	146.6±43.8	83.5±67.8	<0.001	138.3±53.3	89.9±71.3	0.003
Indirect bilirubin level (μmol/L)†	33.9±23.4	61.0±59.9	0.006	52.1±40.1	70.1±71.2	0.226
ALT level (U/L)†	159.7±94.0	80.9±90.8	<0.001	169.0±126.1	102.2±128.2	0.040
AST level (U/L)†	282.3±181.7	149.1±160.8	<0.001	293.4±221.5	172.5±190.3	0.022
GGT level (U/L)†	448.1±261.1	143.8±105.7	<0.001	423.0±273.9	126.7±92.8	<0.001
Albumin level (g/L)†	40.4±3.8	38.1±6.6	0.091	433.3±246.1	353.0±260.9	0.278
ALP level (U/L)†	586.0±211.5	472.6±195.3	0.021	152.8±235.4	169.4±229.2	0.800

†, data are means ± standard deviations, with ranges in square brackets; ‡, data are numbers of patients, with percentages in square brackets; §, P value for the proportion of Kasai types between training cohort and validation cohort. US, ultrasound; BA, biliary atresia; ALT, alanine aminotransferase; AST, aspartate aminotransferase; GGT, γ-glutamyl transferase; ALP, alkaline phosphatase; N/A, not applicable.

the validation cohort. The serum levels of direct bilirubin, ALT, AST, and GGT in the BA group were significantly higher than those in the non-BA group in both the training and validation groups (*Table 1*).

Intraobserver and interobserver reliability

There was almost perfect intraobserver reproducibility of the measurement of the GB abnormality, TC thickness, and liver 2D SWE in each operator, with a kappa of 0.85 (GB abnormality), ICC of 0.95 (TC thickness), and ICC of 0.94 (liver 2D SWE), respectively (all P values <0.001). There was almost perfect agreement between the 2 operators in the measurement of the GB abnormality, TC thickness, and liver 2D SWE. The ICC for TC thickness and liver 2D SWE was 0.99 and 0.99, respectively (both P values <0.001). The kappa for the GB abnormality was 0.77 (P<0.001), which showed substantial interobserver reliability. The Bland-Altman plots also showed agreement between the 2 operators in measuring the TC thickness and liver 2D SWE (Figures S1,S2).

Diagnostic performance of different US parameters, liver 2D SWE, and serum biomarkers in the determination of BA

The AUC of the GB abnormality was 0.82 [95% confidence interval (CI): 0.71–0.87], with a sensitivity of 96% and a specificity of 64% (*Table 2*). The AUC of TC thickness was 0.88 (95% CI: 0.80–0.93). At the cutoff of 2.9 mm, the sensitivity and specificity of the TC thickness were 87% and 88%, respectively (*Table 2*). Other B-mode US parameters had an inferior diagnostic performance in the diagnosis of BA with either a low sensitivity or a low specificity. The AUC of the liver 2D SWE was 0.86 (95% CI: 0.77–0.92). At the cutoff of 8.7 kPa, the sensitivity and specificity of liver 2D SWE were 77% and 83%, respectively (*Table 2*). Among all the serum markers, GGT yielded the highest

Table 2 Diagnostic performance of different US parameters, 2D SWE, serum biomarkers, and nomogram in the diagnosis of biliary atresia in infants younger than 60 days old

US parameters	Cutoff value	AUC[†]	Sensitivity (%)[†]	Specificity (%)[†]	PPV (%)	NPV (%)	Accuracy (%)
B-mode							
GB abnormality	N/A	0.82 (0.71, 0.87)	96 [87, 100]	64 [49, 77]	74	94	81
TC thickness	2.9	0.88 (0.80, 0.93)	87 [75, 95]	88 [76, 96]	89	86	88
Right liver lobe size, cm	7.1	0.87 (0.78, 0.93)	80 [66, 90]	86 [72, 95]	87	79	83
Spleen thickness, cm	1.8	0.74 (0.63, 0.83)	58 [43, 72]	86 [71, 95]	85	61	70
HA diameter, mm	1.8	0.82 (0.70, 0.90)	68 [52, 82]	83 [63, 95]	88	61	74
PV diameter, mm	3.6	0.71 (0.61. 0.80)	90 [78, 97]	51 [36, 66]	67	82	71
SV diameter, mm	2.3	0.75 (0.64, 0.84)	83 [69, 93]	64 [48, 78]	70	79	74
CDFI and PW							
Hepatic subcapsular flow	N/A	0.75 (0.64, 0.84)	63 [47, 78]	86 [72, 95]	81	71	75
HARI	0.77	0.70 (0.58, 0.80)	63 [47, 77]	83 [65, 94]	79	70	73
Liver 2D SWE, kPa	8.7	0.86 (0.77, 0.92)	77 [61, 89]	83 [69, 92]	79	81	80
Serum markers[‡]							
ln (direct bilirubin, μmol/L	79.5	0.79 (0.69, 0.87)	98 [90, 100]	57 [41, 71]	71	96	78
ln (GGT), U/L	255	0.88 (0.80, 0.94)	71 [56, 83]	89 [75, 96]	88	72	79
ln (AST), U/L	142	0.79 (0.70, 0.87)	94 [84, 99]	61 [45, 75]	73	90	78
ln (ALT), U/L	89	0.80 (0.71, 0.87)	80 [67, 90]	76 [61, 87]	79	78	78
Nomogram in training cohort	N/A	0.99 (0.94, 1.00)	92 [78, 98]	100 [91, 100]	100	93	96
Nomogram in validation cohort	N/A	0.98 (0.95, 1.00)	91 [71, 99]	94 [79, 99]	90	94	93

[†], data in parentheses are 95% CIs; [‡], data are the natural logarithm (ln) of the serum biomarker level. US, ultrasound; 2D SWE, 2-dimensional shear wave elastography; AUC, area under the receiver operating characteristic curve; PPV, positive predictive value; NPV, negative predictive value; GB, gallbladder; TC, triangular cord; HA, hepatic artery; PV, portal vein; SV, spleen vein; CDFI, color Doppler flow imaging; PW, pulse wave; HARI, hepatic artery resistive index; ln, natural logarithm; GGT, γ-glutamyl transferase; AST, aspartate aminotransferase; ALT, alanine aminotransferase; N/A, not applicable.

AUC of 0.88 (95% CI: 0.80–0.94), with a sensitivity of 71% and a specificity of 89% (*Table 2*). The AUC of serum ALT was 0.80 (95% CI: 0.71–0.87), with a sensitivity of 80% and a specificity of 76% (*Table 2*).

Development and validation of a nomogram to diagnose BA in infants younger than 60 days old

After multivariable logistic regression analyses and backward step-down selection were completed, GB abnormality, liver 2D SWE, and serum GGT and ALT were selected to establish a nomogram. The GB abnormalities were determined by the US scan protocol (see Methods), serum GGT and ALT levels were converted to the natural logarithm form, and thus, a nomogram was built (*Figure 4*). The sum of points of all 4 parameters was the total points, which directly indicated the probability of BA. The AUC of the nomogram was 0.99 (95% CI: 0.94–1.00; *Figure 5A*), which was significantly higher than all single clinical, US parameters or liver 2D SWE, with a sensitivity of 92% and a specificity of 100% (*Table 2*, Table S1). The calibration curve showed good agreement between the predicted probability and the actual probability in the diagnosis of BA (*Figure 5B*). The DCA curve was conducted to assess the clinical utility of the nomogram and other parameters for the diagnosis of BA. The results showed good clinical utility of the nomogram in predicting BA (*Figure 5C*). The DCA displayed a net benefit of being 52.2% superior to

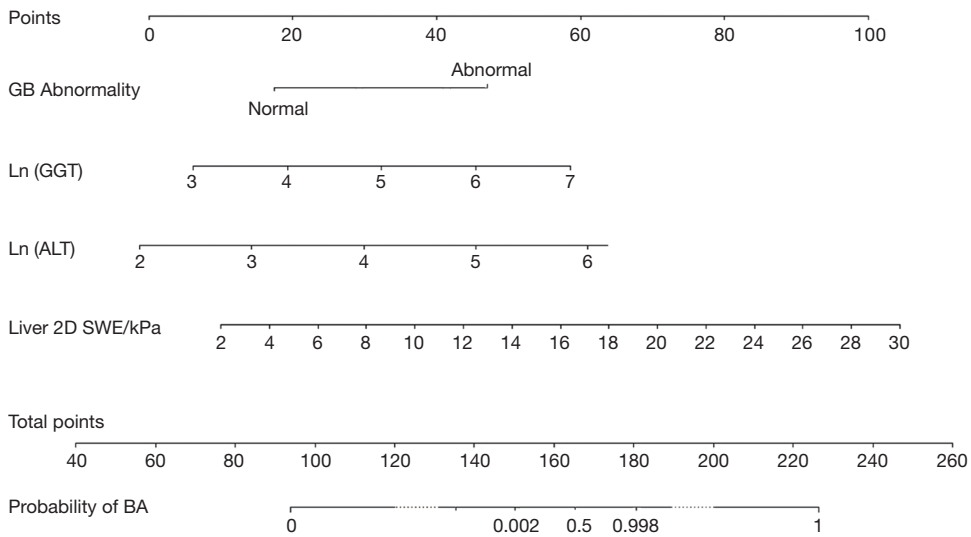

Figure 4 Development of a nomogram to predict the probability of BA using the following 4 predictors: GB abnormality, ln for GGT, ln for ALT, and liver 2D SWE. GB, gallbladder; ln, natural logarithm; GGT, γ-glutamyl transferase; ALT, alanine aminotransferase; 2D SWE, 2-dimensional shear wave elastography; BA, biliary atresia.

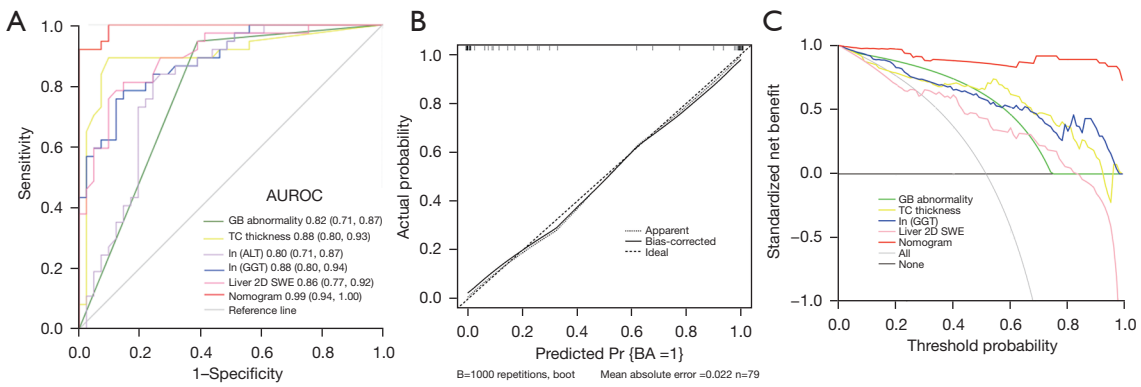

Figure 5 The diagnostic performance characteristics of the nomogram: (A) The AUROC of the nomogram and different parameters. Data in parentheses are 95% CIs. (B) The calibration curve of the nomogram. (C) The DCA curve of the nomogram for BA. AUROC, area under the receiver operating characteristic curve; GB, gallbladder; TC, triangular cord; ln, natural logarithm; ALT, alanine aminotransferase; GGT, γ-glutamyl transferase; 2D SWE, 2-dimensional shear wave elastography; DCA, decision curve analysis; BA, biliary atresia.

TC thickness and 55.9% superior to the natural logarithm (ln; level of GGT) at 80% of the threshold probability (*Figure 5C*, Table S2).

The nomogram in the validation cohort also had good diagnostic performance in the diagnosis of BA, with an AUC of 0.98 (95% CI: 0.95–1.00), a sensitivity of 91%, and a specificity of 94% (*Table 2*). For easy clinical practice, we generated a risk score based on the nomogram, which as calculated as follows: risk score =1.399× liver stiffness measurement (LSM) of SWE + 11.745 × GB abnormality + 5.196 × ln (level of GGT) + 6.462 × ln (level of ALT). In this formula, an abnormal GB =1, and a normal GB =0. A risk score over 0.65 was considered to indicate BA. We also developed a website calculator based on the nomogram in which physicians need only enter the 4 parameters to generate the BA-predicted value directly in the right

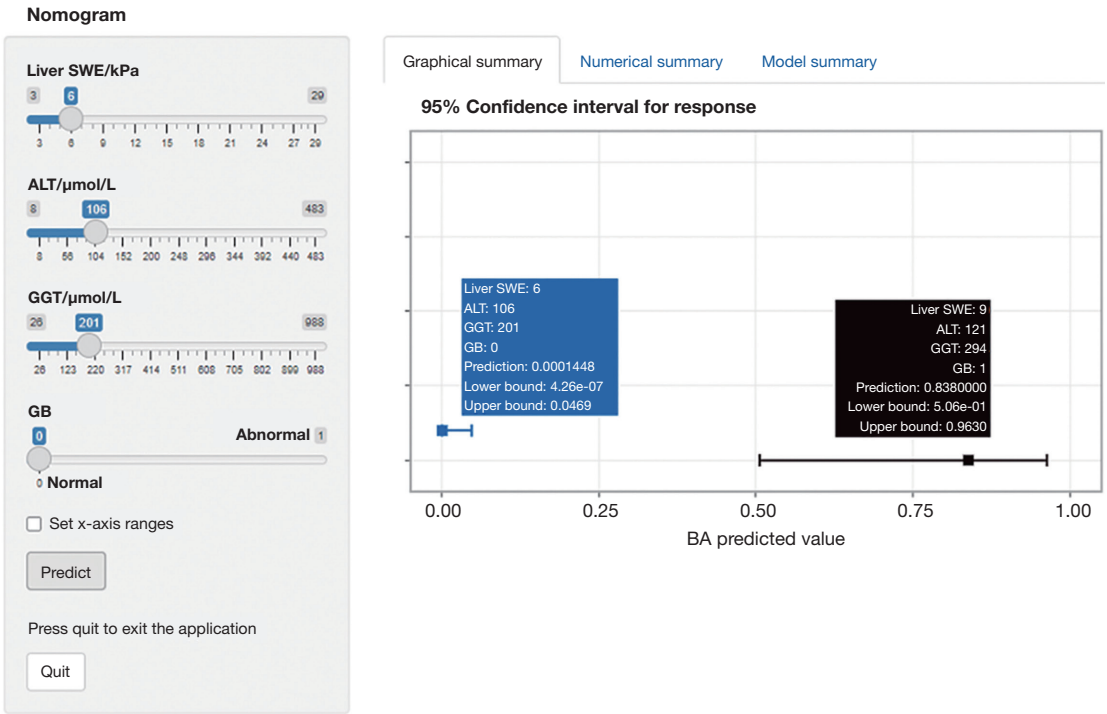

Figure 6 A website calculator to predict biliary atresia: physicians only enter the 4 parameters, and it will generate the predicted value and 95% CI directly in the right window. SWE, shear wave elastography; ALT, alanine aminotransferase; GGT, γ-glutamyl transferase; GB, gallbladder; BA, biliary atresia; CI, confidence interval.

window (*Figure 6*).

Discussion

Timely noninvasive and early diagnosis of BA in young cholestatic infants is still an urgent need for pediatricians and pediatric surgeons. This prospective study developed a novel prediction tool based on a nomogram model for the early diagnosis of BA in young infants using the following 4 predictors: liver 2D SWE, ln for ALT, ln for GGT, and GB abnormalities. This prediction tool yielded an AUC of 0.99 in the training cohort, which was higher than any single clinical, US parameter or liver 2D SWE. This prediction tool had a sensitivity of 92% and a specificity of 100% in the diagnosis of BA in patients aged less than 60 days. This good diagnostic performance was also verified in the validation cohort.

A normal GB in infants should measure over 15 mm with a thin, defined wall in the fasted state (23). According to the practical approach or recent GB classification (9,11), the absence of GB, a small GB with a cutoff length <15 mm, and abnormal shape and wall of GB were defined as GB abnormalities. The detailed definition of abnormal GBs in our prediction tool may facilitate accurate and reliable GB diagnosis.

As patients with BA have persistent neonatal cholestasis and progressive liver fibrosis, younger patients have distinctive US and clinical features compared to older patients. The hemodynamic signs of chronic hepatopathy and portal hypertension on US are reported to be more common in older patients with BA. In one study, hepatic subcapsular flow had 96.3% sensitivity and specificity in predicting BA with a mean age of 68.7 days (24). The HA diameter is significantly smaller in young (younger than 30 days old) infants with BA than in older infants (12). In another study, a follow-up US scan of infants with BA found enlargement of HA diameter and the late presence of signs of portal hypertension on US (12).

Thickening of the TC is also infrequent in young infants with BA. Hwang *et al.* (12) reported that TC thickening was only present in 17% of infants with BA younger than 30 days. Interestingly, they (12) also found thickening of TC during the follow-up of US examination of infants with BA. Due to the progressive liver fibrosis in BA, LSM by 2D SWE

is reported to have a higher diagnostic performance in older BA infants (aged older than 60 days), and LSM is highly positively correlated with age in infants with BA (16,25).

Other studies have obtained similar predictors in the early diagnosis of BA. Wang *et al.* (26) found that GB classification and GGT had good diagnostic performance in identifying BA in patients aged less than 30 days, with an AUC of 0.817. Dillman *et al.* (27) presented a model based on 2D SWE and GGT with an AUC of 0.93 for BA diagnosis in infants younger than 60 days old. Note that the CDFI and PW parameters were not included in the nomogram. Although hepatic subcapsular flow or HARI is useful in BA diagnosis, it is difficult to obtain reliable CDFI and PW results in young, unsedated infants. Meanwhile, the hepatic hemodynamic disturbances in CDFI/PW have been found to be more valuable in identifying portal hypertension for postoperative BA patients compared to early diagnosis (28).

ALT is a sensitive serum marker for hepatocellular injury and an important component of several noninvasive scores for evaluating liver fibrosis, such as Fibrosis-4 score and the AST:ALT ratio. A study of adult patients with chronic hepatitis B showed that ALT affected the results of liver elastography. Dual cutoff values depending on the ALT levels ≤2 × the upper limit of normal (ULN) or >2 × ULN resulted in high accuracy in predicting liver fibrosis (29). Our data showed that liver 2D SWE was significantly positively correlated with the level of serum ALT (r=0.368; P=0.001; Figure S3). Levitte *et al.* and Lee *et al.* also showed that serum ALT significantly positively correlated with the measurement of liver elastography in pediatric liver diseases (30,31). Thus, this new predictor of ALT in our nomogram may adapt the influence of itself and yield a more accurate diagnostic prediction of young BA, but does require further validation.

Serum matrix metalloproteinase 7 (MMP-7) was reported to be a reliable biomarker for BA. Yang *et al.* (32) showed that the diagnostic sensitivity, specificity, and AUC of MMP-7 in differentiating BA from other types of neonatal cholestasis were 98.67%, 95.00%, and 0.99, respectively. Even for diagnosing BA in young infants, MMP-7 yielded an AUC of 0.96 and reflected the severity of liver fibrosis in BA (33). However, due to limited MMP-7 results in our cohort study, we did not include this predictor in our prediction tool.

Our study had several limitations. First, only 104 infants (54 BA and 50 non-BA) and 70 infants (33 BA and 37 non-BA) were included in the training and validation cohorts, respectively. The sample size was relatively small, so we did not analyze the diagnostic performance of the nomogram in patients with BA younger than 30 days old. We will continue further subgroup studies in the future. Second, the detection of GB abnormality might have been affected by the sonographer's experience, although there was high reproducibility. Third, we only used a single manufacturer for 2D SWE, which means that the results and nomogram need to be validated in other 2D SWE equipment from various manufacturers. Fourth, the MMP-7 results of young infants with BA may further optimize our nomogram and we plan to include it in future studies. Finally, the present study was conducted in a single medical center, and validation in different centers is needed. For more versatility and generalizability in clinical practice, we should aim to develop future prediction tools with fewer parameters, such as those without 2D SWE.

In summary, we developed and validated a novel prediction tool to differentiate BA in infants within 60 days from other infant cholestasis, which had good diagnostic performance, sensitivity, and specificity. Prospective validations of this prediction tool in a larger sample sizes and different medical centers are needed in the future, and the early accurate diagnosis of BA will facilitate timely Kasai surgery.

Acknowledgments

Funding: This work was supported by the National Natural Science Foundation of China (No. 82071940) and the Natural Science Foundation of Sichuan Province (No. 2022NSFSC0838).

Footnote

Reporting Checklist: The authors have completed the STARD reporting checklist. Available at https://qims.amegroups.com/article/view/10.21037/qims-22-324/rc

Conflicts of Interest: All authors have completed the ICMJE uniform disclosure form (available at https://qims.amegroups.com/article/view/10.21037/qims-22-324/coif). The authors have no conflicts of interest to declare.

Ethical Statement: The authors are accountable for all aspects of the work in ensuring that questions related to the accuracy or integrity of any part of the work are appropriately investigated and resolved. The study

was conducted in accordance with the Declaration of Helsinki (as revised in 2013). The study was approved by the institutional review board of West China Hospital, Sichuan University, and written informed parental consent was provided by the parents or guardians of all included participants.

References

1. Yoon PW, Bresee JS, Olney RS, James LM, Khoury MJ. Epidemiology of biliary atresia: a population-based study. Pediatrics 1997;99:376-82.
2. Chiu CY, Chen PH, Chan CF, Chang MH, Wu TC; Taiwan Infant Stool Color Card Study Group. Biliary atresia in preterm infants in Taiwan: a nationwide survey. J Pediatr 2013;163:100-3.e1.
3. Sundaram SS, Mack CL, Feldman AG, Sokol RJ. Biliary atresia: Indications and timing of liver transplantation and optimization of pretransplant care. Liver Transpl 2017;23:96-109.
4. Karrer FM, Lilly JR, Stewart BA, Hall RJ. Biliary atresia registry, 1976 to 1989. J Pediatr Surg 1990;25:1076-80; discussion 1081.
5. Serinet MO, Wildhaber BE, Broué P, Lachaux A, Sarles J, Jacquemin E, Gauthier F, Chardot C. Impact of age at Kasai operation on its results in late childhood and adolescence: a rational basis for biliary atresia screening. Pediatrics 2009;123:1280-6.
6. Okubo R, Nio M, Sasaki H; Japanese Biliary Atresia Society. Impacts of Early Kasai Portoenterostomy on Short-Term and Long-Term Outcomes of Biliary Atresia. Hepatol Commun 2021;5:234-43.
7. Fawaz R, Baumann U, Ekong U, Fischler B, Hadzic N, Mack CL, McLin VA, Molleston JP, Neimark E, Ng VL, Karpen SJ. Guideline for the Evaluation of Cholestatic Jaundice in Infants: Joint Recommendations of the North American Society for Pediatric Gastroenterology, Hepatology, and Nutrition and the European Society for Pediatric Gastroenterology, Hepatology, and Nutrition. J Pediatr Gastroenterol Nutr 2017;64:154-68.
8. Lee HJ, Lee SM, Park WH, Choi SO. Objective criteria of triangular cord sign in biliary atresia on US scans. Radiology 2003;229:395-400.
9. Zhou LY, Wang W, Shan QY, Liu BX, Zheng YL, Xu ZF, Xu M, Pan FS, Lu MD, Xie XY. Optimizing the US Diagnosis of Biliary Atresia with a Modified Triangular Cord Thickness and Gallbladder Classification. Radiology 2015;277:181-91.
10. Humphrey TM, Stringer MD. Biliary atresia: US diagnosis. Radiology 2007;244:845-51.
11. Napolitano M, Franchi-Abella S, Damasio MB, Augdal TA, Avni FE, Bruno C, Darge K, Ključevšek D, Littooij AS, Lobo L, Mentzel HJ, Riccabona M, Stafrace S, Toso S, Woźniak MM, Di Leo G, Sardanelli F, Ording Müller LS, Petit P. Practical approach to imaging diagnosis of biliary atresia, Part 1: prenatal ultrasound and magnetic resonance imaging, and postnatal ultrasound. Pediatr Radiol 2021;51:314-31.
12. Hwang SM, Jeon TY, Yoo SY, Choe YH, Lee SK, Kim JH. Early US findings of biliary atresia in infants younger than 30 days. Eur Radiol 2018;28:1771-7.
13. Yang L, Ling W, He D, Lu C, Ma L, Tang L, Luo Y, Chen S. Shear wave-based sound touch elastography in liver fibrosis assessment for patients with autoimmune liver diseases. Quant Imaging Med Surg 2021;11:1532-42.
14. Galina P, Alexopoulou E, Mentessidou A, Mirilas P, Zellos A, Lykopoulou L, Patereli A, Salpasaranis K, Kelekis NL, Zarifi M. Diagnostic accuracy of two-dimensional shear wave elastography in detecting hepatic fibrosis in children with autoimmune hepatitis, biliary atresia and other chronic liver diseases. Pediatr Radiol 2021;51:1358-68.
15. Chen H, Zhou L, Liao B, Cao Q, Jiang H, Zhou W, Wang G, Xie X. Two-Dimensional Shear Wave Elastography Predicts Liver Fibrosis in Jaundiced Infants with Suspected Biliary Atresia: A Prospective Study. Korean J Radiol 2021;22:959-69.
16. Zhou LY, Jiang H, Shan QY, Chen D, Lin XN, Liu BX, Xie XY. Liver stiffness measurements with supersonic shear wave elastography in the diagnosis of biliary atresia: a comparative study with grey-scale US. Eur Radiol 2017;27:3474-84.
17. Sandberg JK, Sun Y, Ju Z, Liu S, Jiang J, Koci M, Rosenberg J, Rubesova E, Barth RA. Ultrasound shear wave elastography: does it add value to gray-scale ultrasound imaging in differentiating biliary atresia from other causes of neonatal jaundice? Pediatr Radiol

2021;51:1654-66.
18. Chen Y, Zhao D, Gu S, Li Y, Pan W, Zhang Y. Three-color risk stratification for improving the diagnostic accuracy for biliary atresia. Eur Radiol 2020;30:3852-61.
19. Feldman AG, Sokol RJ. Neonatal cholestasis: emerging molecular diagnostics and potential novel therapeutics. Nat Rev Gastroenterol Hepatol 2019;16:346-60.
20. Wang Y, Jia LQ, Hu YX, Xin Y, Yang X, Wang XM. Development and Validation of a Nomogram Incorporating Ultrasonic and Elastic Findings for the Preoperative Diagnosis of Biliary Atresia. Acad Radiol 2021;28 Suppl 1:S55-63.
21. Lee MS, Kim MJ, Lee MJ, Yoon CS, Han SJ, Oh JT, Park YN. Biliary atresia: color doppler US findings in neonates and infants. Radiology 2009;252:282-9.
22. Dietrich CF, Bamber J, Berzigotti A, Bota S, Cantisani V, Castera L, Cosgrove D, Ferraioli G, Friedrich-Rust M, Gilja OH, Goertz RS, Karlas T, de Knegt R, de Ledinghen V, Piscaglia F, Procopet B, Saftoiu A, Sidhu PS, Sporea I, Thiele M. EFSUMB Guidelines and Recommendations on the Clinical Use of Liver Ultrasound Elastography, Update 2017 (Long Version). Ultraschall Med 2017;38:e16-47.
23. Brahee DD, Lampl BS. Neonatal diagnosis of biliary atresia: a practical review and update. Pediatr Radiol 2022;52:685-92.
24. El-Guindi MA, Sira MM, Konsowa HA, El-Abd OL, Salem TA. Value of hepatic subcapsular flow by color Doppler ultrasonography in the diagnosis of biliary atresia. J Gastroenterol Hepatol 2013;28:867-72.
25. Liu Y, Peng C, Wang K, Wu D, Yan J, Tu W, Chen Y. The utility of shear wave elastography and serum biomarkers for diagnosing biliary atresia and predicting clinical outcomes. Eur J Pediatr 2022;181:73-82.
26. Wang G, Zhang N, Zhang X, Zhou W, Xie X, Zhou L. Ultrasound characteristics combined with gamma-glutamyl transpeptidase for diagnosis of biliary atresia in infants less than 30 days. Pediatr Surg Int 2021;37:1175-82.
27. Dillman JR, DiPaola FW, Smith SJ, Barth RA, Asai A, Lam S, Campbell KM, Bezerra JA, Tiao GM, Trout AT. Prospective Assessment of Ultrasound Shear Wave Elastography for Discriminating Biliary Atresia from other Causes of Neonatal Cholestasis. J Pediatr 2019;212:60-65.e3.
28. Gu LH, Fang H, Li FH, Zhang SJ, Han LZ, Li QG. Preoperative hepatic hemodynamics in the prediction of early portal vein thrombosis after liver transplantation in pediatric patients with biliary atresia. Hepatobiliary Pancreat Dis Int 2015;14:380-5.
29. Zeng J, Zheng J, Jin JY, Mao YJ, Guo HY, Lu MD, Zheng HR, Zheng RQ. Shear wave elastography for liver fibrosis in chronic hepatitis B: Adapting the cut-offs to alanine aminotransferase levels improves accuracy. Eur Radiol 2019;29:857-65.
30. Levitte S, Lee LW, Isaacson J, Zucker EJ, Milla C, Barth RA, Sellers ZM. Clinical use of shear-wave elastography for detecting liver fibrosis in children and adolescents with cystic fibrosis. Pediatr Radiol 2021;51:1369-77.
31. Lee JE, Ko KO, Lim JW, Cheon EJ, Song YH, Yoon JM. Correlation between Transient Elastography (Fibroscan®) and Ultrasonographic and Computed Tomographic Grading in Pediatric Nonalcoholic Steatohepatitis. Pediatr Gastroenterol Hepatol Nutr 2022;25:240-50.
32. Yang L, Zhou Y, Xu PP, Mourya R, Lei HY, Cao GQ, Xiong XL, Xu H, Duan XF, Wang N, Fei L, Chang XP, Zhang X, Jiang M, Bezerra JA, Tang ST. Diagnostic Accuracy of Serum Matrix Metalloproteinase-7 for Biliary Atresia. Hepatology 2018;68:2069-77.
33. Wu JF, Jeng YM, Chen HL, Ni YH, Hsu HY, Chang MH. Quantification of Serum Matrix Metallopeptide 7 Levels May Assist in the Diagnosis and Predict the Outcome for Patients with Biliary Atresia. J Pediatr 2019;208:30-37.e1.

Cite this article as: Yan H, Liu J, Jin S, Du L, Wang Q, Luo Y. A novel prediction tool based on shear wave elastography, gallbladder ultrasound, and serum biomarkers for the early diagnosis of biliary atresia in infants younger than 60 days old. Quant Imaging Med Surg 2023;13(1):259-270. doi: 10.21037/qims-22-324

Supplementary

Table S1 Comparison of AUCs between nomogram and other diagnostic markers

US features & SWE	Cutoff value	AUC[†]	P value[‡]
GB abnormality	N/A	0.82 (0.71, 0.87)	<0.001
TC thickness/mm	2.9	0.88 (0.80, 0.93)	0.02
Liver SWE	8.7	0.86 (0.77, 0.92)	0.01
ln (GGT)	255	0.88 (0.80, 0.94)	0.002
ln (ALT)	89	0.80 (0.71, 0.87)	<0.001
Nomogram	0.65	0.99 (0.94, 1.00)	N/A

[†], Data are numbers of participants, with percentages in parentheses. [‡], P values are compared with the AUC of nomogram using DeLong's test. ALT, alanine aminotransferase, AUC, area under the receiver operating characteristic curve, BA, biliary atresia; GB, gallbladder; GGT, γ-glutamyl transferase; SWE, shear wave elastography; TC, triangular cord.

Table S2 Decision curve analysis of the nomogram

Threshold probability	Standardized net benefit (%)[†]				
	GB abnormality	TC thickness	ln (GGT)	Liver 2D SWE	Nomogram
0.1	92.6 (87.3, 97.3)	87.0 (82.5, 93.7)	92.6 (87.2, 95.6)	86.3 (79.9, 91.9)	97.9 (94.8, 100.0)
0.2	88.0 (78.6, 94.1)	78.7 (70.5, 89.3)	82.8 (73.4, 90.9)	69.9 (56.9, 85.9)	97.3 (88.5, 100.0)
0.3	82.0 (70.4, 90.3)	72.5 (59.2, 86.0)	73.1 (59.6, 85.7)	65.6 (37.4, 79.9)	88.4 (83.3, 100.0)
0.4	74.1 (58.7, 85.8)	70.4 (52.5, 85.2)	65.4 (48.6, 80.1)	61.5 (25.2, 75.5)	88.3 (79.8, 100.0)
0.5	63.0 (41.3, 79.3)	66.7 (52.2, 84.5)	58.8 (40.4, 76.6)	43.6 (2.6, 68.0)	86.5 (76.3, 100.0)
0.6	46.3 (12.8, 70.5)	62.0 (38.3, 81.7)	52.0 (29.8, 71.2)	35.9 (-9.1, 59.5)	83.8 (75.0, 100.0)
0.7	18.5 (0, 57.0)	47.5 (20.0, 73.2)	43.8 (14.2, 66.0)	22.2 (-15, 56.2)	91.9 (76.9, 100.0)
0.8	0 (0, 0.218)	37.0 (-1.8, 64.4)	33.3 (11.5, 63.0)	5.1 (-26.3, 51.2)	89.2 (72.9, 100.0)
0.9	0 (0, 0)	13.0 (-31.3, 55.6)	35.3 (6.5, 57.4)	-15.4 (-50.0, 48.5)	89.2 (64.6, 100.0)

[†], Data in parentheses are 95% CIs. GB, gallbladder; GGT, γ-glutamyl transferase; 2D SWE, 2-dimensional shear wave elastography; TC, triangular cord; ln, natural logarithm.

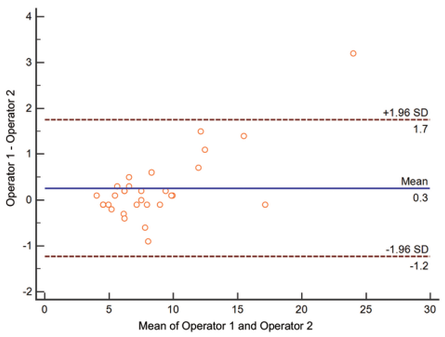

Figure S1 Bland-Altman plots of interobserver agreement between 2 operators in the measurement of liver 2D SWE. 2D SWE, 2-dimensional shear wave elastography; SD, standard deviation.

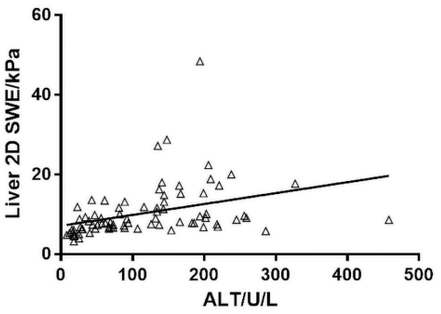

Figure S3 Pearson correlation showed that there was a significant positive correlation between liver 2D SWE and the level of serum ALT (r=0.368; P=0.001). 2D SWE, 2-dimensional shear wave elastography; ALT, alanine aminotransferase.

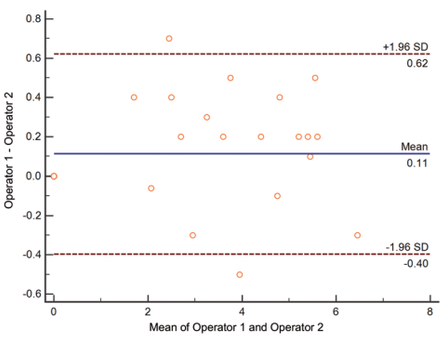

Figure S2 Bland-Altman plots of interobserver agreement between 2 operators in the measurement of TC thickness. TC, triangular cord; SD, standard deviation.

https://dx.doi.org/10.21037/qims-22-324